IEEE Access
Multidisciplinary | Rapid Review | Open Access Journal

Received April 24, 2020, accepted May 18, 2020, date of publication May 21, 2020, date of current version June 4, 2020.

Digital Object Identifier 10.1109/ACCESS.2020.2996509

The Influence of DC Component on the Creepage Discharge Paths in Oil-Pressboard Insulation Under AC-DC Combined Voltage

PENG ZHOU, GUANGNING WU, (Senior Associate Member), BO GAO, YAN YANG, GUANGCAI HU, AND CHENG LIU

School of Electrical Engineering, Southwest Jiaotong University, Chengdu 611756, China

Corresponding author: Yan Yang (yangyanyy@home.swjtu.edu.cn)

This work was supported by the National Key Research and Development Program of China under Grant 2017YFB0902704.

ABSTRACT The main dielectric medium in converter transformers is the oil-pressboard. The valve windings of converter transformers are subjected to AC-DC combined voltage. Creepage discharge is a common defect of oil-pressboard insulation. The degree of the oil-immersed pressboard (OIP) damage is directly affected by different creepage discharge paths. In this study, a needle-plate model was developed to explore different creepage discharge paths in oil-pressboard insulation under AC-DC combined voltage. A high-speed camera was used to record the developmental process of white marks on the OIP. We explored reasons behind the different creepage discharge paths under different voltage types. Results revealed that the creepage discharge path and the degree of OIP damage were influenced by the DC component. Although the damaged OIP in converter transformers may cause catastrophic flashover inside the transformers, it is difficult to replace it. This implies that transformer insulation designers should pay attention to the influence of the DC component on OIP damage. In this study, we used pulse current method to detect discharge patterns. Discharge parameters were then extracted from discharge patterns. We observed that developmental process of white marks corresponded to developmental process of discharge parameters. This suggests that creepage discharges can be diagnosed based on discharge parameters. Based on these conclusions, important information was provided for the on-line monitoring design of transformer insulation status.

INDEX TERMS Converter transformer, AC-DC combined voltage, DC component, creepage discharge, white mark.

I. INTRODUCTION

Converter transformers operate under much complex operating conditions compared to traditional AC transformers. The valve windings of converter transformers are subjected to AC-DC combined voltage. The performance of such transformers is directly related to the safety operations of the power grid [1]. Of note, failure rate of converter transformers is about twice that of AC transformers. According to the statistics published by the international organization of power grids (CIGRE), insulation faults account for nearly half of all faults [2]. Creepage discharges that develop along the surface and inner layers of the OIP cause irreparable damage to the insulating properties of the OIP [3]. However, it is difficult to replace damaged OIP in converter transformers. The degree of OIP damage is directly affected by different creepage discharge paths. This calls for the need to study the influence of DC component on the creepage discharge path in oil-pressboard insulation under AC-DC combined voltage.

Creepage discharge contributes to failure of oil-pressboard insulation. This discharge is aggravated when the insulation structure of converter transformers is complex, the distribution of DC field and AC field is different and the conductivity of oil and pressboards varies nonlinearly with the intensity of electric field and temperature [4]. These factors make it impossible to avoid strong tangential electric field in the local insulation structure in converter transformers such as those in the sides of spacers and strips, the local area of end angled rings and the overlapping area of the cylinder pressboards. Strong tangential electric field easily leads to creepage discharges. Currently, the column-plate model [5]–[7] and the needle-plate model [8]–[11] are used

The associate editor coordinating the review of this manuscript and approving it for publication was Jenny Mahoney.

to simulate the creepage discharge under different electric fields. The needle-plate model is divided into two structures. In the first structure, the needle electrode is perpendicular to the OIP. It is used to determine partial discharges in the inner layers of the OIP [8]. In the second structure, the needle electrode is parallel to the OIP. It is used to determine creepage discharges at the surface layer of the OIP [11]. Different defective discharges can be characterized based on discharge patterns [12], time-frequency characteristics [13] and gas-generation characteristics [5].

Dendritic deterioration marks are often detected on damaged transformers. These marks are derived from prior white marks [14]. White marks compromise the performance and structure of OIP leading to breakdown of OIP. However, white marks disappear when they come into contact with the air. Therefore, white marks are hardly observed when transformers are maintained. It has been reported that even if white marks disappear from the OIP, the original channels created by the white marks continue to extend as the voltage is increased [15]. The same study used the needle-plate model to explore the development of white marks under AC voltage. They recorded the developmental process of white marks using a high-speed camera as well as the damage caused by creepage discharges to the OIP [11]. Another study analyzed creepage discharges and white marks using the needle-plate model under AC-DC combined voltage. They found that there was no white mark on the OIP [16]. Hence, they could not explain the dendritic deterioration marks on damaged transformers. On the other hand, due to the demand for reverse transmission power of the power system, dielectric medium in converter transformers is subjected to the DC component with different polarities under different operating conditions. It is imperative to explore the development of creepage discharges under the action of DC components with different polarities.

In this study, we explored the developmental process of creepage discharges in oil-pressboard insulation under AC-DC combined voltage and compared it with the creepage discharges under AC voltage. The needle-plate model was designed and a high-speed camera was used to record the formation and developmental process of white marks on the OIP. Moreover, we observed that developmental process of white marks corresponded to developmental process of discharge parameters recorded by the discharge detector. We also analyzed the influence of DC component on the creepage discharge path. The depth of carbonized marks on the OIP was measured by a confocal laser scanning microscope (CLSM). Finally, the influence of different voltage types on the degree of OIP damage was compared and analyzed.

II. EXPERIMENTAL SETUP

A. EXPERIMENTAL SAMPLE AND ELECTRODE

The transformer oil used in this study was KI50X. The oil was first heated to 60 °C and then filtered through a vacuum oil filter for 2 hours to remove moisture, particulate matters and gases. The parameters of the filtered transformer oil are shown in Table 1.

TABLE 1. Main properties of the filtered transformer oil.

Property	Quality Index	Actual Value	Experimental Standard (China)
Moisture content (mg/kg)	≤30/40	20	GB/T 7600-2014
Breakdown voltage (kV)	≥42	65	GB/T 507-2002
Dielectric dissipation factor (90 ^{0}C)	≤0.005	0.0007	GB/T 5654-2007
Interfacial tension (mN/m)	≥40	47	GB/T 6541-1986
Acid value (mg/g)	≤0.01	0.006	0836-2010 NB/SH/T

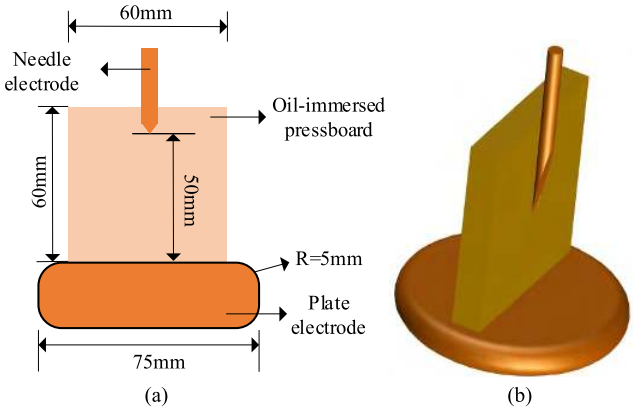

FIGURE 1. The needle-plate electrodes model. (a) dimension figure. (b) 3D figure.

The pressboards (1 mm thickness) were first cut into the specifications shown in Fig.1(a). They were then dried at 105 °C for 48 hours to remove moisture. Next, They were vacuum dried at 85 °C and 50 Pa for 24 hours to remove gases. The pressboards were then completely immersed in an oil tank filled with oil in a vacuum at 85 °C and 50 Pa for 48 hours. This procedure produced fully impregnated pressboard samples with moisture levels around 0.3% by weight [17].

The shape of the needle tip was semi-conical to ensure that the needle and OIP fitted properly. The curvature radius of the front of the needle tip was 27-28 μm while its side was 14-15 μm. An insulation support was used to fix the OIP. The OIP was perpendicular to the plate electrode to ensure that the needle electrode, OIP and plate electrode were integrated (Fig.1).

B. EXPERIMENTAL CIRCUIT AND PROCEDURE

In this study, the discharge from the samples was detected by using the pulse current method. The transformers used in these experiments were all partial discharge free transformers discharging at less than 5 pC at 200 kV. C_1 and C_2 constituted the voltage divider. MPD600 served as the discharge detector set at a frequency range of 0∼20 MHz. I SPEED TR was used to record the phenomenon on the OIP during the experiments. The equipment was shoot at a frequency of up to 10000 fps (Fig.2). During the design and construction of the platform, measures were taken to suppress

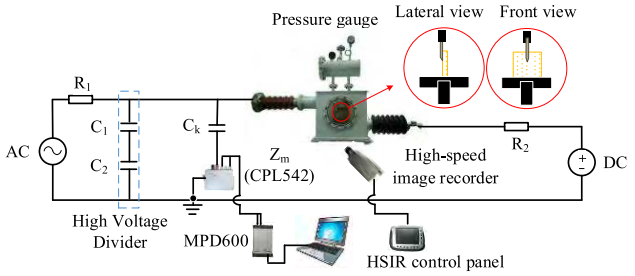

FIGURE 2. Diagram of the experimental setup. R_1-protective resistance, 90 KΩ; R_2-protective resistance, 2 MΩ; Z_m-measuring impedance; C_k-coupling capacitance, 300 pF.

corona interference. The high voltage leads were made of smooth and polished aluminum guide rods. This caused all connectors to be chamfered without a tip or spike. In the whole system, the interference of partial discharges was below 10 pC at $100_{RMS} + 100$ kV.

The AC and DC voltages were respectively applied to the side of the sample [18]–[20]. The needle electrode was connected to the AC voltage application system while the plate electrode was connected to the DC voltage application system. The ripple factor (RF) of AC-DC combined voltage is defined by equation (1), where U_{DC} is the DC value and U_{AC} is the AC root mean square (RMS) value.

$$RF = U_{AC}/U_{DC} \tag{1}$$

The RF of AC-DC combined voltage depends on the connection mode of windings of the converter transformer and the number of bridge rectifiers [21]. This study aimed to explore the converter transformers used in high-voltage direct current transmission system with two bridge rectifiers, where the RFs were approximately 1 and 1/3. To explore the influence of polarities of the DC component on creepage discharge paths, $RF = \pm 1$ were taken as examples ($RF = +1$ meant applying positive DC component while $RF = -1$ meant applying negative DC component).

The DC field takes 20 minutes to stabilize [22]. Therefore, the DC voltage was preloaded for 20 minutes and then the AC voltage was superimposed. Once the AC voltage was superimposed, it was stabilized for 4 minutes. Next, the discharge parameters were recorded for 1 minute to represent the discharge parameters within 25 (20 + 4 + 1) minutes. The creepage discharge behavior at various voltages was examined by using the step-up stress method. The steps used were 2 kV, and $2_{RMS} \pm 2$ kV ($AC_{RMS} \pm$ DC). In summary, voltages were increased by 2kV every 25 minutes. Voltages were kept constant when white marks appeared. Next, discharge parameters were recorded every 10 minutes until the breakdown on the OIP occurred and the experiment was terminated. The step-up voltage method was used to not only obtain a large amount of experimental data and phenomena within a short time but also obtain results similar to that of the constant voltage method.

In the experiments, the timing was started when the AC voltage was 22 kV. This ensured that discharges were generated at the needle electrode under different voltage types. For convenient comparisons, the value of the pure AC voltage was equal to the value of the AC component in the AC-DC combined voltage at the same time. Ten experiments were completed under each voltage type to eliminate the influence of errors caused by needle deflection, grooves on pressboard surface and random discharge. Averaged values of ten experiments were computed and used for subsequent analyses and comparisons.

III. EXPERIMENTAL RESULTS

A. CHARACTERISTICS OF CREEPAGE DISCHARGES

The characteristics of creepage discharges in oil-pressboard insulation were characterized by discharge parameters Qpeak and frequency (f). The discharge parameters were calculated automatically by MPD600 during the experiment and displayed in real-time. Parameters were defined as:

Q: The value of the apparent charge.

Qpeak: The maximum amplitude of apparent charge value.

f: The frequency of creepage discharges.

In Fig.3, the value of the pure AC voltage was (22 + t/12.5) kV before white marks appeared (The first peak). The voltage was kept constant when white marks appeared. Moreover, the value of the pure AC voltage was equal to the value of the AC component in the AC-DC combined voltage at the same time. Qpeak was characterized by four stages: the slow increase stage (1), the stage with rapid increase followed by a decline (2), the stable development stage (3) and the leaping increase stage (4) (Fig.3a). f was characterized by two stages: the slow increase stage (1) and the fast increase stage (2) (Fig.3b). Similar trends for Qpeak and f were observed under AC-DC combined voltage and under AC voltage. This observation implies that the discharge stage division under AC voltage was still applicable under AC-DC combined voltage. However, the Qpeak value under AC-DC combined voltage was greater than the Qpeak value under AC voltage (Fig.3a) while the f value under AC-DC combined voltage was less than the f value under AC voltage (Fig.3b).

MPD600 was used to record the discharge patterns. The cumulative discharge number in a minute was collected for each pattern. The denser the points, the higher the number of discharges. Based on thirty experiments, it was discovered that the developmental process of discharge patterns under AC-DC combined voltage was similar with that under AC voltage. When the $RF = -1$ voltage was applied, discharge patterns showed different characteristics at different discharge stages (Fig.4). Before white marks generation, Q and f values were small. The Q values were mainly concentrated in the first and third quadrants (Fig.4a). When white marks appeared, the shape of the discharge pattern was like the rabbit ear (Fig.4b). Next, Qpeak values decreased while f values increased. The Q values were mainly between 100 pC and 1000 pC (Fig.4c). At the adjacent flashover moment, the discharges reached a full phase and the Q values

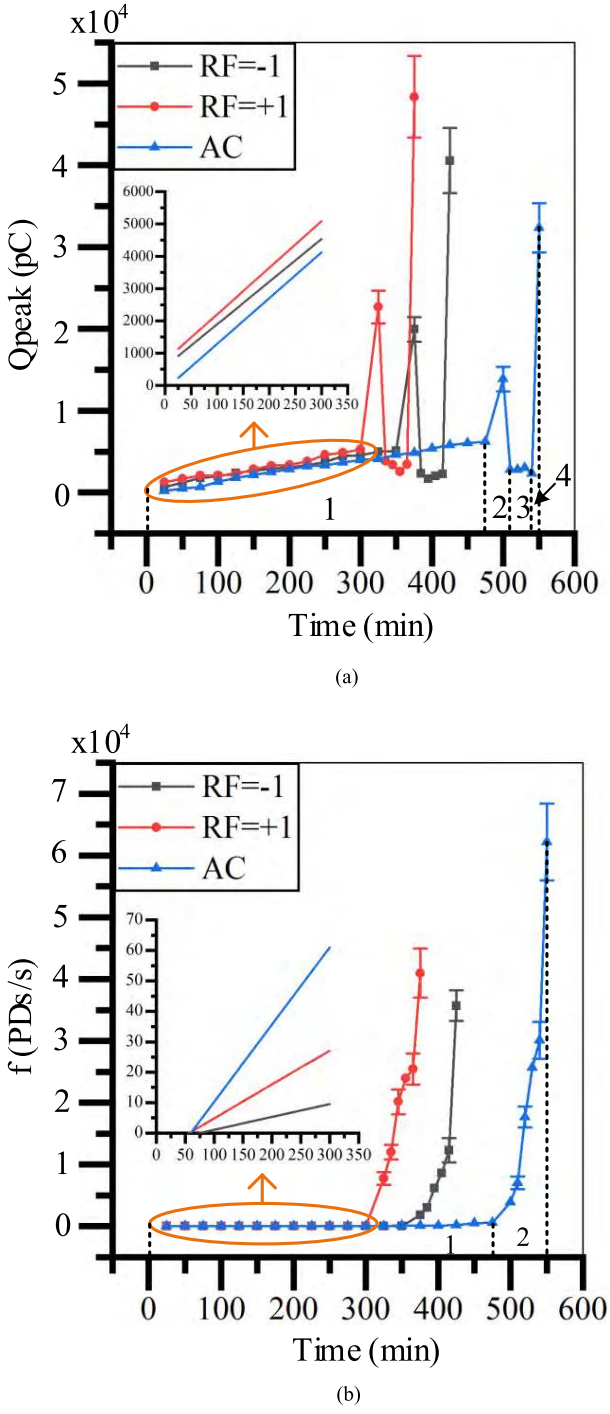

FIGURE 3. The developmental process of discharge parameters under different voltage types. (a) the developmental process of Qpeak. (b) the developmental process of f.

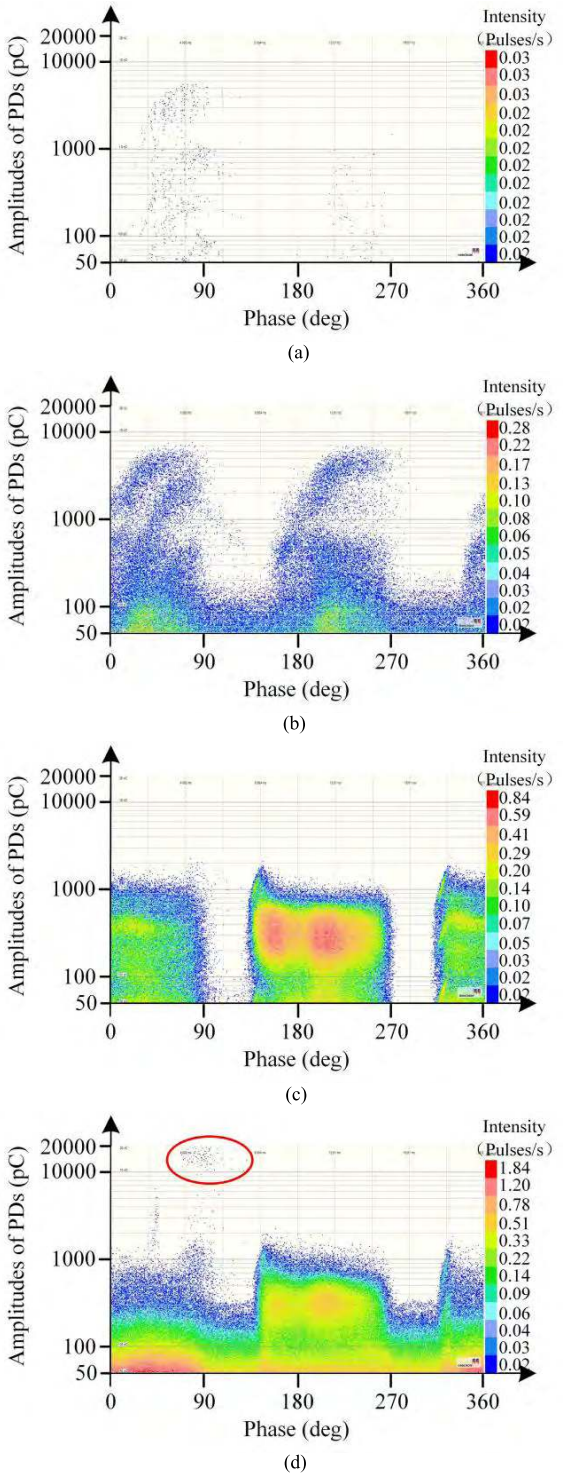

FIGURE 4. The developmental process of discharge patterns under RF = −1 voltage. (a) the pattern at 350 minutes (50_{RMS} − 50 kV). (b) the pattern at 375 minutes (52_{RMS} − 52 kV). (c) the pattern at 400 minutes (52_{RMS} − 52 kV). (d) the pattern at 425 minutes (52_{RMS} − 52 kV).

(over 10 nC) concentrated around 90° (In red circle position of Fig.4d).

B. DEVELOPMENTAL PROCESS OF THE WHITE MARK

A high-speed camera was used to record the formation and developmental process of the OIP in real-time. The developmental processes of white marks were similar under the AC-DC combined voltage and the AC voltage. The RF = −1 voltage resulted to white marks at a frequency of spark sharped discharges of 120 times/minute (Fig.5a). The stable discharge channel developed from a single chan-

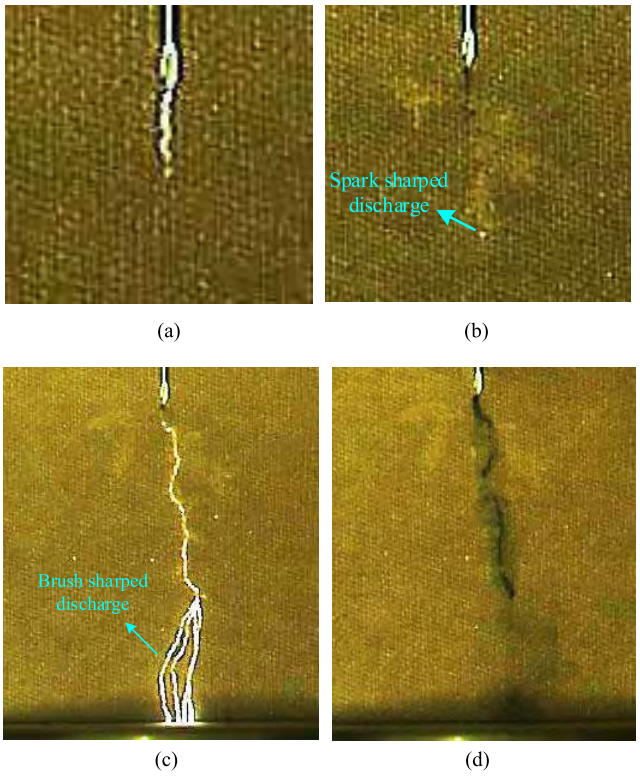

FIGURE 5. The developmental process of the white mark under RF = −1 voltage (52_{RMS} - 52 kV). (a) the generation of the white mark. (b) the development of the white mark. (c) the flashover moment. (d) the carbonized marks after the breakdown.

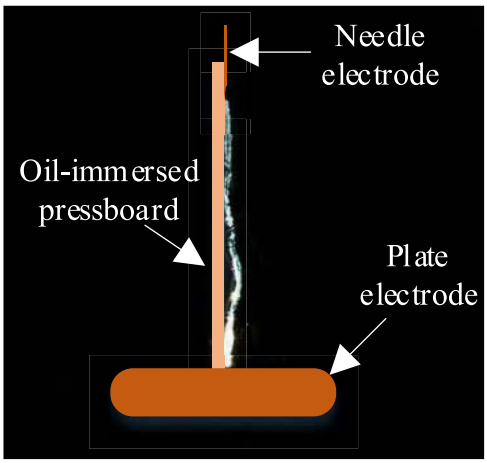

FIGURE 6. The side view at flashover time.

nel to a dendritic channel (Fig.5b). The white mark slowly extended to the plate electrode, and the spark sharped discharge no longer occurred at the needle electrode. However, the weak spark sharped discharges appeared at the white mark endpoint. At the flashover moment, brush sharped discharges were generated between the white mark endpoint and the plate electrode (Fig.5c). This implied that the creepage discharge path was transferred from the OIP to the oil (Fig.6). After the breakdown on the OIP, the carbonized

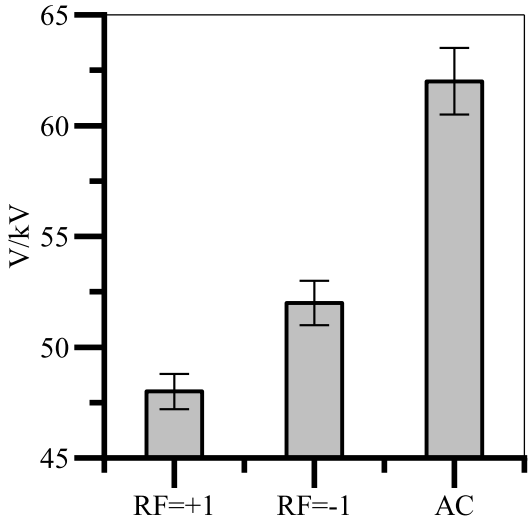

FIGURE 7. The initial voltage of white marks under different voltage types.

marks were produced on the OIP along the flashover path. However, the degree of OIP damage in the brush sharped discharge area was significantly less than that in the white mark area (Fig.5d).

When the RF = +1 voltage was applied, the initial voltage of the white mark was 48_{RMS} + 48 kV while it was 52_{RMS} −52 kV when the RF = −1 voltage was applied. In the same line, when the AC voltage was applied, the initial voltage of the white mark was 62 kV (Fig.7).

Application of different voltage types resulted to different creepage discharge paths. When the RF = −1 voltage was applied, the white mark extended 35mm (Fig.8a) causing the brush sharped discharges to go off the OIP (Fig.6) followed by flashover. On the other hand, when the AC voltage was applied, the white mark extended 45mm causing the brush sharped discharges (Fig.8b). However, when the RF = +1 voltage was applied, no brush sharped discharge occurred. The white mark extended to the plate electrode while flashover occurred between the needle electrode and the plate electrode through the white mark paths (Fig.8c). Compared with creepage discharges under the AC voltage, the negative DC component transferred the creepage discharge paths from the OIP to the oil. However, the positive DC component kept the creepage discharge paths on the OIP.

C. THE DEGREE OF OIP DAMAGE

To explore the degree of OIP damage under different voltage types, the depths of carbonized marks on the OIP were measured by CLSM. The OIP carbonized marks were 350 μm, 550 μm and 250 μm when AC voltage, RF = +1 voltage and RF = −1 voltage were applied respectively (Fig.9). These experimental results indicated that positive DC component increased the degree of OIP damage compared with the degree of OIP damage under AC voltage. However, negative DC component reduced the degree of OIP damage.

IV. DISCUSSION

A. THE RELATIONSHIP BETWEEN DEVELOPMENTAL PROCESS OF WHITE MARKS AND DISCHARGE PARAMETERS

The development of white marks was diagnosed by monitoring the discharge parameters in the actual operation of the converter transformer. The developmental process of white marks corresponded to the developmental process of discharge parameters. On applying RF = −1 voltage, the pattern before white marks generation corresponded to the discharge parameters recorded at 350 minutes (Fig.4a). White mark formation corresponded to the discharge parameters recorded at 375 minutes (Fig.4b). Development of white marks corresponded to the discharge parameters recorded at 400 minutes (Fig.4c) while the adjacent flashover moment corresponded to the discharge parameters recorded at 425 minutes (Fig.4d).

The discharge parameters showed a significant variation trend at different stages of creepage discharges under AC-DC combined voltage. These variations reflected the developmental process of creepage discharges from the side. They could also be used to predict and evaluate the insulation state of the oil-pressboard insulation.

B. DC COMPONENT DEPENDENT CREEPAGE DISCHARGE PATH

In order to measure the surface potential of the OIP, additional experiments were performed. The power was turned off during the white mark developmental process. The areas at white mark endpoint were then measured 10 times by an electrometer under each voltage type. The surface potentials were negative. Results showed that the bubbles attached to the white mark endpoint mainly had negative charges. The explanation for the bubbles mainly having negative charges could have been due to presence of both positive and negative ions caused by ionization. The peak value of the alternating electric field intensity produced by the needle electrode was much higher than that of the electrostatic field intensity produced by the plate electrode. Therefore, the movement of the charge was mainly affected by the needle electrode (The alternating electric field). When the AC voltage applied to the needle electrode was the negative half cycle, the needle electrode injected electrons into the bubbles and neutralized the positive ions. At this point, the negative ions and electrons remained in the bubbles. When the AC voltage applied on the needle electrode was the positive half cycle, the electrons and negative ions in the bubbles could have been affected by the forces of electric field thus migrating to the needle tip. However, the migration rates of negative ions are much lower than that of electrons. The mobility of negative ions is 1×10^{-9} $m^2/V{\cdot}s$ while that of electrons is 1×10^{-4} $m^2/V{\cdot}s$ [23]. Therefore, the negative ions could not complete the migration in half a cycle and thus remained in the bubbles.

When the negative DC voltage was applied to the plate electrode, the bubbles were simultaneously affected by the upward buoyancy forces F_b and electric field forces F_e in the vertical direction (Fig.10a). When the plate electrode was grounded, bubbles were only affected by the upward buoyancy forces F_b (Fig.10b). Further, when the positive DC

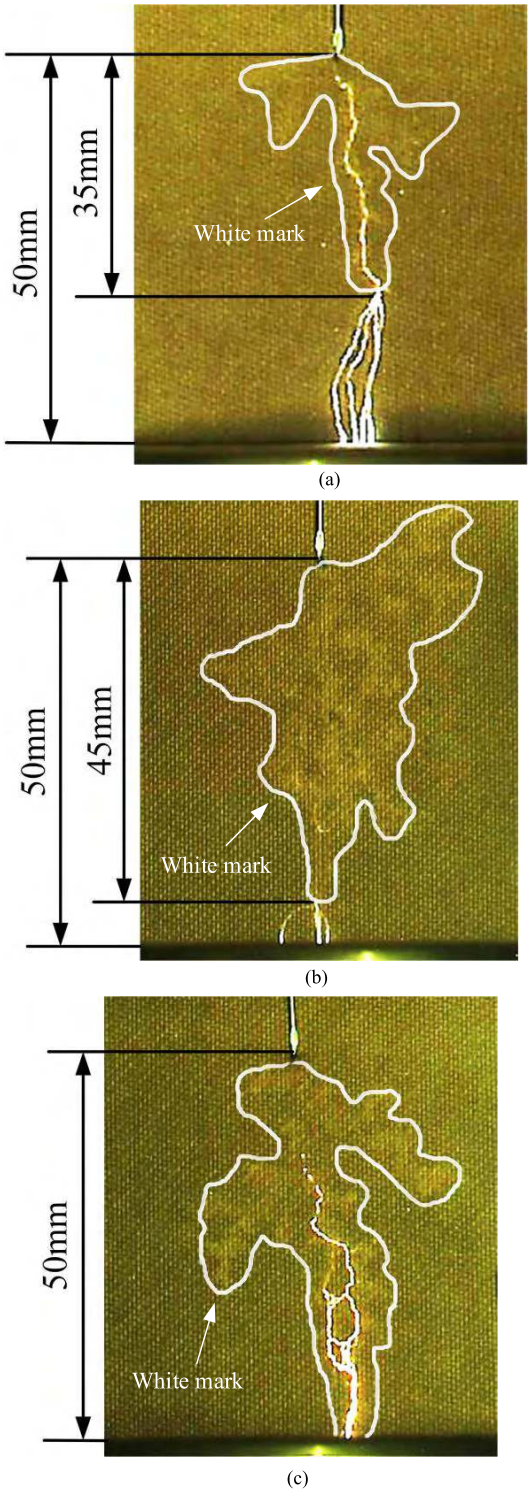

FIGURE 8. The creepage discharge paths near flashover moment under different voltage types. (a) the creepage discharge path under RF = −1 voltage (52_{RMS} - 52 kV). (b) the creepage discharge path under the AC voltage (62kV). (c) the creepage discharge path under RF = +1 voltage (48_{RMS}+ 48 kV).

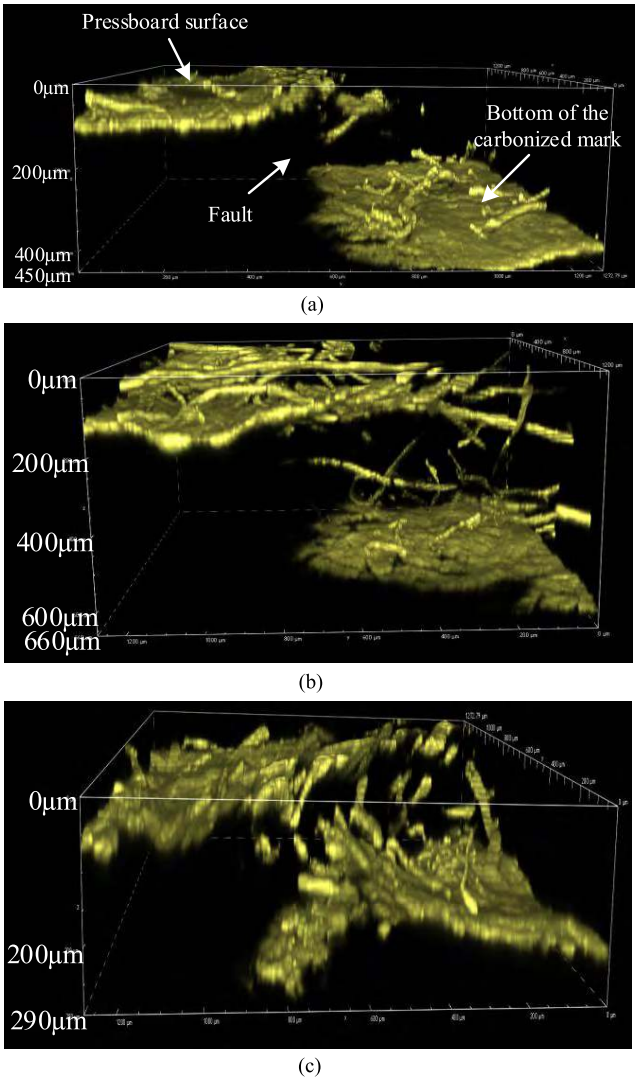

FIGURE 9. The depth of carbonized marks on the OIP under different voltage types. (a) the depth of carbonized marks under the AC voltage (62kV). (b) the depth of carbonized marks under RF = +1 voltage (48_{RMS}+ 48 kV). (c) the depth of carbonized marks under RF = −1 voltage (52_{RMS} - 52 kV).

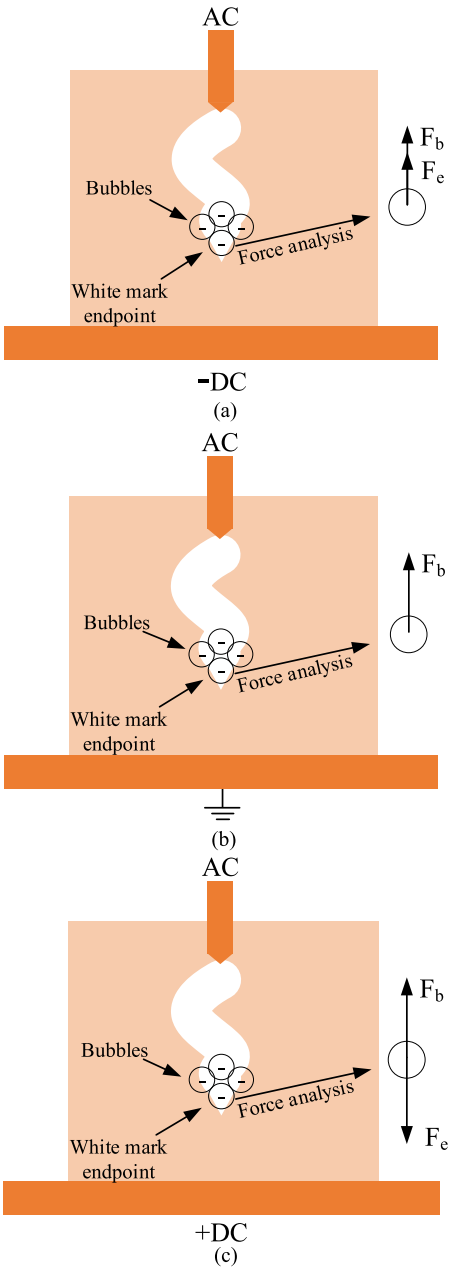

FIGURE 10. The behavior of bubbles at the white mark endpoint under different voltage types. (a) RF = −1 voltage was applied. (b) the AC voltage was applied. (c) RF = +1 voltage was applied.

voltage was applied to the plate electrode, the bubbles were affected by the upward buoyancy forces F_b and downward electric field forces F_e(Fig.10c). Creepage discharge is intermittent. Before the next discharge, the bubbles at the white mark endpoint were few when the RF = −1 voltage was applied, slightly more when the AC voltage was applied but many when the R = +1 voltage was applied.

COMSOL Multiphysics 5.4 was used to simulate the system to know the value of the electric field intensity required to produce white marks. The sizes of the simulation model were consistent with the experimental model. Oil and pressboards parameters used are shown in Table 2 [16]. The influence of space charges was not considered in the electric field simulation. As shown in Fig.7, the initial voltage of white marks under the AC voltage was 62 kV. Moreover, when 62 kV AC voltage was applied and the plate electrode was grounded, the maximum electric field intensity at the needle tip was 926 kV/mm (Fig.11). It indicated that 926 kV/mm might be the minimum electric field intensity required to produce white marks during creepage discharges at the oil-pressboard interface. During the developmental process of white marks, flashover in the oil occurred if the electric field intensity at the white mark endpoint was high enough to break the insulation oil between the white mark endpoint and the plate electrode. However, the insulation oil between the white mark endpoint and the plate electrode remained intact

TABLE 2. Material parameters for electric field distribution simulations.

Material	ε_r	γ (S/m)
Transformer oil	2.2	$6.56\text{x}10^{-14}\cdot\exp(0.279E)$
OIP	4.2	$1.69\text{x}10^{-14}\cdot\exp(0.023E)$

if many bubbles were present. The low electric field intensity breakdown characteristics of bubbles produced a shielding effect and weakened the electric field intensity at the white mark endpoint.

In summary, when the R $= -1$ voltage was applied, the bubbles at the white mark endpoint were few thus causing minimal shielding effect. When the AC voltage was applied, the bubbles were slightly more thus causing an increased shielding effect compared to that caused by R $= -1$ voltage. When the R $= +1$ voltage was applied, the bubbles were many thus causing even a greater shielding effect compared to the other two types of voltage. Further, application of R $= -1$ voltage caused a high electric field intensity at the white mark endpoint thus increasing the probability of flashover in the oil to occur. However, application of R $= +1$ voltage caused the opposite of this to occur. Notably, application of AC voltage caused intermediate effects.

C. DC COMPONENT DEPENDENT DEGREE OF OIP DAMAGE

Previous studies revealed that charges accumulated on the OIP had the same polarity as the electrode [24], [25]. Therefore, when the negative DC voltage was applied to the plate electrode, negative charges accumulated on the inside and back surface of the OIP to form the space electric field. The bubbles were subjected to electric field forces pointing outside of the OIP further leaving the OIP (The white mark in Fig.6a is lighter than that in Fig.6c). Therefore, the bubbles on the OIP under the RF $= -1$ voltage were less compared to those under the AC voltage. This reduced creepage discharges in the bubbles resulting in a reduced degree of OIP damage. When the positive DC voltage was applied to the plate electrode, positive charges accumulated on the inside and back surface of the OIP to form the space electric field. The bubbles were subjected to electric field forces pointing inside of the OIP thus developing into the OIP. Therefore, the bubbles on the OIP under the RF $= +1$ voltage were more compared to those under the AC voltage. This enhanced the creepage discharges in bubbles resulting in an increased degree of OIP damage.

The surface transport of charges caused discharges along the surface of the OIP contributing to surface flashover. The bulk transport of charges caused discharge into the OIP thus causing damage to OIP. The electric fields at the needle tip were along the surface of the OIP thus causing most of the charges to constitute the surface transport and a small number of charges to constitute the bulk transport. The DC component weakened the electric field intensity in the opposite direction and strengthened the electric field intensity in the same

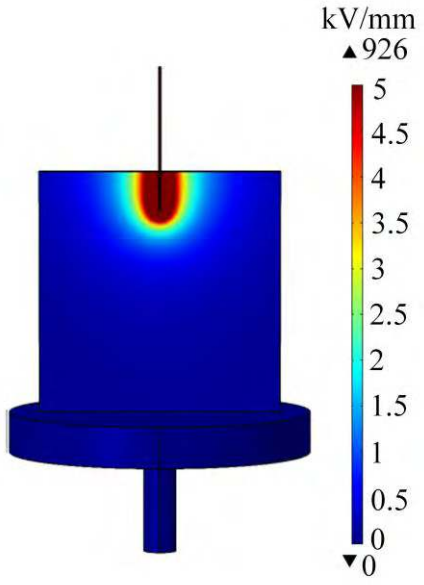

FIGURE 11. The electric field distribution under the AC voltage. (62kV, $\phi = 90°$).

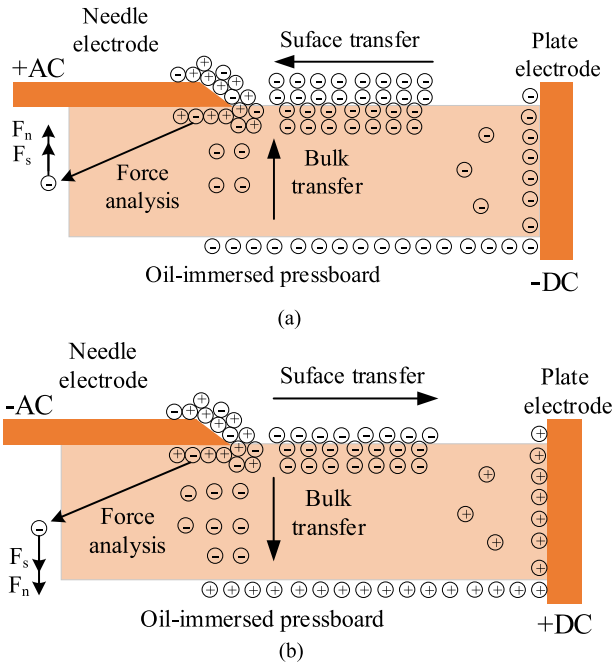

FIGURE 12. The schematic diagram of charge transport characteristics under different voltage types. (a) RF $= -1$ voltage was applied. (b) RF $= +1$ voltage was applied.

direction of the alternating electric field. Therefore, the concern was the moment when the polarity of the AC component was opposite to that of the DC component. The charge transport model is shown in Fig. 12. When the negative DC voltage was applied to the plate electrode, negative charges accumulated on the inside and back surface of the OIP to form the space electric field. Negative charges generated by

ionization were affected by the electric field force F_s of space electric field and the electric field force F_n of the needle electrode. The charges participating in the bulk transfer were less compared with the charges under the AC voltage thus reducing the damage inside the OIP. When the positive DC voltage was applied to the plate electrode, positive charges accumulated on the inside and back surface of the OIP to form the space electric field. Negative charges generated by ionization and injected by the needle electrode were affected by the electric field force F_s of space electric field and the electric field force F_n of the needle electrode. Compared with the charges under the AC voltage, more charges were involved in the bulk transfer aggravating the damage inside the OIP.

V. CONCLUSION

In this study, the needle-plate model was used to study creepage discharge paths in oil-pressboard insulation under different voltage types. Based on the results and discussion, several conclusions are drawn.

1) The discharge stage division under AC voltage is still applicable under AC-DC combined voltage. The creepage discharge stage can be divided into four stages: initial stage of discharges, initial stage of creepage discharges, development stage of creepage discharges and pre-breakdown stage.
2) The developmental process of creepage discharge corresponds to the developmental process of discharge parameters. This makes it possible to diagnose the insulation state of the transformer by monitoring discharge parameters.
3) The DC component affects the creepage discharge paths. The negative DC component makes flashover in the oil more likely to occur compared with the paths under the AC voltage. This causes the creepage discharge paths to move from the OIP to the oil in advance. On the other hand, the positive DC component makes the creepage discharge to occur along the surface of OIP.
4) The DC component affects the degree of OIP damage. The negative DC component decreases the degree of OIP damage compared with the damage of the OIP under the AC voltage. On the other hand, the positive DC component increases the degree of OIP damage.

REFERENCES

[1] X. Sun, Z. H. Liu, L. Y. Gao, and Y. G. Ding, "Practice and innovation in the ±800 kV UHVDC demonstration project," *Proc. CSEE*, vol. 29, no. 22, pp. 35–45, Aug. 2009.
[2] *In Service Performance of HVDC Converter Transformers and Oil-cooled Smoothing Reactors, Electra*, CIGRE, Paris, France, 1994.
[3] *HVDC LCC Converter Transformers Converter Transformer Failure Survey Results From 2003 to 2012*, CIGRE, Paris, France, 2015.
[4] A. Kurita, E. Takahasi, J. Ozawa, M. Watanabe, and K. Okuyana, "DC flashover voltage characeteristics and their calculation method for oil-immersed insulation systems in HVDC transformers," *IEEE Trans. Power Del.*, vol. PWRD-1, no. 3, pp. 184–190, Jul. 1986.
[5] B. Qi, Z. Wei, and C. Li, "Creepage discharge of oil-pressboard insulation in AC-DC composite field: Phenomenon and characteristics," *IEEE Trans. Dielectr. Electr. Insul.*, vol. 23, no. 1, pp. 237–245, Feb. 2016.
[6] *Electrical Strength of Insulating Materials Test Methods*, Standard 60243-1998, IEC, Geneva, Switzerland, 1998.
[7] X. Li, Z. Huang, J. Li, T. Jiang, M. A. Mehmood, and S. Hou, "Phenomenon analysis and state classification of surface discharge on oil-impregnated pressboard under AC-DC combined voltage," *AIP Adv.*, vol. 8, no. 10, Oct. 2018, Art. no. 105023.
[8] Y. Sha, Y. Zhou, L. Zhang, M. Huang, and F. Jin, "Measurement and simulation of partial discharge in oil-paper insulation under the combined AC–DC voltage," *J. Electrostatics*, vol. 71, no. 3, pp. 540–546, Jun. 2013.
[9] Y. Sha, Y. Zhou, J. Li, and J. Wang, "Partial discharge characteristics in oil-paper insulation under combined AC-DC voltage," *IEEE Trans. Dielectr. Electr. Insul.*, vol. 21, no. 4, pp. 1529–1539, Aug. 2014.
[10] X. Chen, J. Hao, R. Liao, J. Li, L. Yang, and D. Feng, "AC surface flashover and gas generation difference of the cellulose insulation pressboard immersed in novel 3-Element mixed oil and mineral oil," *IEEE Access*, vol. 7, pp. 147048–147059, 2019.
[11] G. C. Hu, G. N. Wu, R. Yu, P. Zhou, B. Gao, Y. Yang, and K. Liu, "The influence of pressure on the discharge along oil-paper interface under AC stress," *Energies*, vol. 12, no. 10, pp. 1846–1862, May 2019.
[12] Y. Zhang, J. Tang, C. Pan, and X. Luo, "Comparison of PD and breakdown characteristics induced by metal particles and bubbles in flowing transformer oil," *IEEE Access*, vol. 7, pp. 48098–48108, 2019.
[13] A. H. El-Hag, Y. A. Saker, and I. Y. Shurrab, "Online oil condition monitoring using a partial- discharge signal," *IEEE Trans. Power Del.*, vol. 26, no. 2, pp. 1288–1289, Apr. 2011.
[14] X. Yi and Z. D. Wang, "The influences of solid surface on the propagation of creepage discharge in insulating liquids," *IEEE Trans. Dielectr. Electr. Insul.*, vol. 22, no. 1, pp. 303–312, Feb. 2015.
[15] X. Yi and Z. Wang, "Surface tracking on pressboard in natural and synthetic transformer liquids under AC stress," *IEEE Trans. Dielectr. Electr. Insul.*, vol. 20, no. 5, pp. 1625–1634, Oct. 2013.
[16] X. Li, J. Li, T. Jiang, Y. Wang, and Z. Huang, "Analysis of creeping discharges on oil-impregnated pressboard under combined AC and DC voltages," *IEEE Trans. Dielectr. Electr. Insul.*, vol. 25, no. 6, pp. 2380–2388, Dec. 2018.
[17] J. Dai, Z. Wang, and P. Jarman, "Creepage discharge on insulation barriers in aged power transformers," *IEEE Trans. Dielectr. Electr. Insul.*, vol. 17, no. 4, pp. 1327–1335, Aug. 2010.
[18] B. Qi, Z. Wei, C. R. Li, X. H. Zhang, F. Li, and H. B. wang, "Discharge characteristics of the typical defects in oil-paper insulation under AC–DC compound voltage," *High Voltage Eng.*, vol. 41, no. 2, pp. 639–646. Feb. 2015.
[19] S. Li, W. Si, and Q. Li, "Partition and recognition of partial discharge development stages in oil-pressboard insulation with needle-plate electrodes under combined AC-DC voltage stress," *IEEE Trans. Dielectr. Electr. Insul.*, vol. 24, no. 3, pp. 1781–1793, Jun. 2017.
[20] Y. L. Cheng, B. Qi, C. R. Li, and C. C. Xi, "Impact of interfacial charge of oil-pressboard insulation on surface flashover voltage under compound AC–DC electric field," *Power Syst. Technol.*, vol. 38, no. 4, pp. 1070–1075, Apr. 2014.
[21] L. Bao, J. Li, J. Zhang, X. Li, and X. Li, "Influences of temperature on partial discharge behavior in oil-paper bounded gas cavity under pulsating DC voltage," *IEEE Trans. Dielectr. Electr. Insul.*, vol. 23, no. 3, pp. 1482–1490, Jun. 2016.
[22] B. Qi, Y. L. Cheng, C. R. Li, C. C. Xi, and S. Q. Zhang, "Characteristics of interface charge on oil-impregnated pressboard under non-uniform AC-DC combined electric field," *Proc. CSEE*, vol. 33, no. 34, pp. 241–249, Dec. 2013.
[23] F. M. O'Sullivan, "A model for the initiation and propagation of electrical streamers in transformer oil and transformer oil based nanofluids," Ph.D. dissertation, Dept. Elect. Eng., MIT, Boston, MA, USA, 2007.
[24] Y. Zhou, Y. Wang, G. Li, N. Wang, Y. Liu, B. Li, P. Li, and H. Cheng, "Space charge phenomena in oil-paper insulation materials under high voltage direct current," *J. Electrostatics*, vol. 67, nos. 2–3, pp. 417–421, May 2009.
[25] C. Tang, G. Chen, M. Fu, and R. J. Liao, "Space charge behavior in multi-layer oil-paper insulation under different DC voltages and temperatures," *IEEE Trans. Dielectr. Electr. Insul.*, vol. 17, no. 3, pp. 778–788, Jun. 2010.

PENG ZHOU was born in Zhejiang, China, in 1996. He received the B.Eng. degree from Southwest Jiaotong University, Chengdu, in 2018, where he is currently pursuing the M.E. degree. His research interests include condition monitoring, fault diagnosis, and insulation life-span evaluation for electrical equipment.

GUANGNING WU (Senior Associate Member) was born in Nanjing, China, in July 1969. He received the B.Sc., M.Sc., and Ph.D. degrees in electrical engineering from Xi'an Jiaotong University, in 1991, 1994, and 1997, respectively. He is currently a Professor with the School of Electrical Engineering, Southwest Jiaotong University. His research interests include condition monitoring, fault diagnosis, and insulation life-span evaluation for electrical equipment.

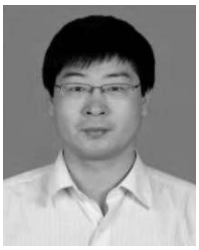

BO GAO was born in Hebei, China, in 1976. He received the B.Sc. and M.Sc. degrees in electrical engineering from Southwest Jiaotong Unversity, in 2000 and 2003, respectively. He is currently an Associate Professor with the School of Electrical Engineering, Southwest Jiaotong University. His research interest includes condition detection and fault diagnosis of electrical equipment, including oil-filled power transformers and generators.

YAN YANG was born in Sichuan, China, in 1984. She received the B.Sc. and Ph.D. degrees in electrical engineering from Xi'an Jiaotong University, in 2005 and 2010, respectively. From 2010 to 2015, she was with the State Grid Chongqing Electric Power Research Institution, China. She is currently a Lecturer with the School of Electrical Engineering, Southwest Jiaotong University. Her research interest includes dielectrical properties of functional materials and condition diagnosis.

GUANGCAI HU was born in Hubei, China, in 1981. He received the B.Sc. and M.Sc. degrees in electrical engineering from Zhengzhou University, in 2005 and 2008, respectively. He is currently pursuing the Ph.D. degree in high-voltage and insulation technology with the School of Electrical Engineering, Southwest Jiaotong University. His research interests include insulation condition diagnosis and state evaluation of power transformers.

CHENG LIU was born in Sichuan, China, in 1995. He received the B.Sc. degree in electrical engineering from the Harbin University of Science and Technology, in 2018. He is currently pursuing the M.Sc. degree in electrical engineering with the School of Electrical Engineering, Southwest Jiaotong University. His research interests include properties of oil-pressboard insulation under high-temperature, moisture content, and inhomogeneous electrical field.